Organics on Mars : Laboratory studies of organic material under simulated martian conditions

Kate, Inge Loes ten

Chapter 5

Analysis and survival of amino acids in martian regolith analogues

We have investigated the native amino acid composition of two analogues of martian soil, JSC Mars-1 and Salten Skov. A Mars simulation chamber has been built and used to expose samples of these analogues to temperature and lighting conditions similar to those found at low-latitudes on the martian surface. The effects of the simulated conditions have been examined using high performance liquid chromatography (HPLC). Exposure to energetic ultraviolet (UV) light in vacuum appears to cause a modest increase in the concentration of certain amino acids within the materials, which is interpreted as resulting from the degradation of microorganisms. The influence of low temperatures shows that the accretion of condensed water on the soils leads to the destruction of amino acids, supporting the idea that reactive chemical processes involving H_2O are at work within the martian soil. We discuss the influence of UV radiation, low temperatures and gaseous CO_2 on the intrinsic amino acid composition of martian soil analogues and describe, with the help of a simple model, how these studies fit within the framework of life detection on Mars and the practical tasks of choosing and using martian regolith analogues in planetary research.

James R. C. Garry, Inge Loes ten Kate, Zita Martins, Per Nørnberg, Pascale Ehrenfreund
Meteoritics and Planetary Science; accepted 26 Ocober 2005

1. INTRODUCTION

Mars' current atmospheric pressure is too low to allow pure liquid water to persist at its surface – liquid water will freeze and evaporate. Data from orbiters and rovers (Haskin *et al.*, 2005, Squyres *et al.*, 2004a,b) indicate that liquid water has been present in significant amounts on Mars in the past, possibly allowing biologically important reactions to occur (Squyres, 1984). The question of whether life arose on Mars has therefore been widely discussed in the planetary community, since the conditions in its early history may have resembled those of the early Earth by having a dense atmosphere and persistent liquid water at its surface (McKay, 1997). However, a combination of energetic UV radiation, the extreme dryness and the presumed oxidising nature of the soil make Mars' present surface an inhospitable place for terrestrial organisms. Organic matter carried by impacting meteorites appears to be affected by the same processes. The Viking Mars landers attempted to detect organic molecules in the upper surface three decades ago, but no evidence was found for organic matter that was not already present at low levels within the spacecraft's analysis equipment (Biemann *et al.*, 1977). However, the lower detection limit of the Pyrolysis Release experiment of Viking would not have detected bacterial communities numbering in the millions per gram (Klein, 1978). Thus, while many mechanisms have been proposed to explain the overall negative response of the Viking experiments, it is possible that organic matter may have present but at concentrations lower than could be detected by the equipment.

An international effort of Solar System exploration will lead to several space missions that will search for extinct or extant life on Mars during the next decade. In this context it is vital to obtain knowledge about the survival of organic material exposed to martian conditions. Laboratory simulations provide a convenient path to understanding chemical reactions on the martian surface and studies have shown that there are a number of processes, both photochemical and photolytic, that reproduce aspects of the biological results of Viking, a summary of which can be found in Klein (1978). It is known that pure amino acids can be destroyed by exposure to UV light with a spectrum similar to that found at the surface of Mars and the rate of degradation is high relative to geological timescales (ten Kate *et al.*, 2005; Stoker and Bullock, 1997). Unshielded glycine and D-alanine molecules have half-lives of the order of 10^4 to 10^5 s under noontime conditions at the martian equator (ten Kate *et al.*, 2005). More complex molecules are expected to be altered either by photolytic or photochemical pathways. Of particular interest is the role that water might play, either through the formation of gaseous oxidising agents in the atmosphere, or when chemisorbed into minerals or present as thin quasi-liquid films. Of particular interest is the role that water might play, either in the formation of gaseous oxidising agents in the atmosphere, or in similar oxidising reactions when chemisorbed into minerals or present as thin quasi-liquid films on mineral surfaces.

In this paper we report data on the native amino acid content of martian analogues using HPLC coupled with UV fluores-

cence detection. This technique is well-suited to the analysis of complex mixtures of organic matter and by using this method we have quantified the native amino acid content of the Mars-1 material from Johnson Space Center (JSC), and a Danish soil (Salten Skov), both of which are internationally used martian soil simulants. These materials were then exposed within a specially designed cryogen-cooled simulation chamber to conditions of temperature, UV lighting and pressure, that are similar to those on Mars. The composition and properties of the martian soil analogues are discussed in section 2 and the HPLC analyses are described in section 3. Our experimental simulations are outlined in section 4 with the results summarised in section 5. We then discuss the implications of these martian simulations in the context of future exploration efforts to detect organic molecules in the martian subsurface.

2. Regolith analogues

The two materials used in this study have different physical characteristics and mineralogy. It is not our intent to examine the broader view of how the degradation rate of organic matter varies with the general properties of regoliths such as grain size or mineralogy. Instead, by using materials that are available to the planetary science community, we provide information about these soil analogues that can be used for disciplines ranging from planetary protection to material compatibility tests, among others. Characteristics of each analogue are summarised briefly in the following sections.

2.1 JSC Mars-1

A martian soil analogue, hereafter referred to as Mars-1, is available to the research community from JSC. It is an ochre-coloured mixture of weathered volcanic ash collected from the Pu'u Nene cinder cone, located in the saddle between the Mauna Loa and Mauna Kea volcanoes on the island of Hawaii (Allen *et al.*, 1998). This soil approximates the composition, grain size, density, and magnetic properties of martian soil and has been used in a number of Mars-oriented research studies that examine physical (Sternovsky *et al.*, 2002) and biological processes (Kral *et al.*, 2004). The elemental abun-

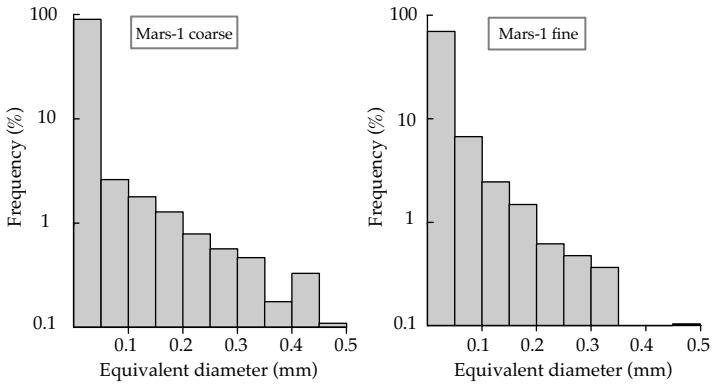

Fig. 1. The frequency distribution of grain diameters in two samples of the Mars-1 regolith.

dances of the Mars-1 material are broadly similar to that inferred from Viking surface studies although the degree to which its mineralogy is comparable to that of martian surface is not well known. Optical microscopic imaging of the powder shows irregular unweathered grains and computer analysis of these images, by the NIH Image software package, was used to find the distribution of grain cross-sections. From these data, an effective grain diameter distribution was calculated using the assumption that the grains were substantially spherical and the resulting data are shown in Fig. 1.

The broad range of grain sizes in the Mars-1 material causes a significant degree of self-sorting. This leads to a segregation of the material based on grain size. Additionally, it is possible that different mineralogies are present in the largest and smallest fractions of the material. Thus, two sub-samples were prepared from the bulk supply of Mars-1, one made up of the larger grains, and one predominantly containing the smaller grains. This separation was achieved by gentle shaking of approximately 500 g of the original material in a polyethylene bag and such action is intended to replicate the agitation that might occur in transit or in simple handling of the bulk material. No contamination-control documents were available for the two types of analogue used, and it is therefore possible that they contained organic material such as plasticisers, that had migrated from plastic scoops, bags, and similar handling tools. The extent to which such contamination might occur is limited, since the presented area of the regolith powders (>100 m^2 per kg) is far larger than the internal area (~500 cm^2) of the smallest bag used in these experiments.

2.2 Salten Skov

This dark red Danish soil, named after its source in the central Jutland region, is rich in precipitates of iron oxides and is excavated from an area on the scale of several hundred m^2. To date, this analogue has had limited use in martian simulation studies, with emphasis placed on its fine grain size and magnetic properties. A mineralogical study of this analogue has been made (Nørnberg *et al.*, 2004) but as yet the localised nature of the soil and its chemical nature are not well understood. The silt and clay size fraction (< 63 μm) used in this

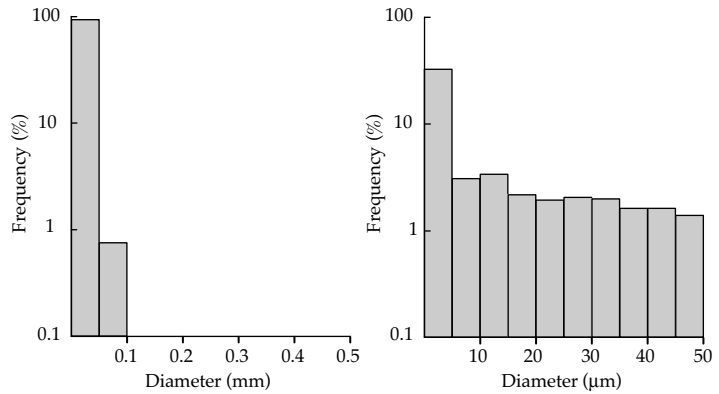

Fig. 2. Showing the grain size distributions of the Salten Skov material used.

experiment makes up 35.5 % of the particles smaller than 2 mm. This fraction was separated from the total sample by dry sieving. It has a free iron content of 35.8 % of which nearly 90 % is crystalline iron oxides (DCB/Oxalate extraction). Most of the grains with a diameter < 63 μm consist of aggregates, which can be split into particles ~2 μm in size. The particle size of the < 63 μm fraction was determined by laser diffraction and the particle size distribution is seen in Fig. 2, which shows two charts of the same data. The leftmost chart uses the same scale as was used to plot the Mars-1 grain size data in Fig. 1, and illustrates the complete absence of particles with diameters larger than 0.2 mm. The second chart in Fig. 2 shows the same data as the left-most chart, but plotted over one tenth of the physical scale, showing that the Salten Skov material is composed predominantly of dust-size particles.

2.3 Control material

The extent to which cross-contamination of the samples occurred within the irradiation chamber was monitored by the use of a third material. This control sample was a quantity of finely crushed Pyrex. It was expected that accidental transport of grains during the use of the chamber's pumping equipment, or sublimation and recondensation of the amino acids when in vacuum, might be observed by the detection of novel compounds in the Pyrex at the end of the experiment.

3. Experiments and Methods

3.1 Samples

All of the samples were separately ground into powder in a glove box purged with argon gas, and were stored in sterilised glass vials before being used in the experiments. An unused Pyrex test tube was crushed into powder and then heated to 500 °C for 3 hours for use as a reference blank, using the same process as for the samples.

3.2 Chemicals and reagents

All tips and Eppendorf tubes used in this work were sterilised. All tools, glassware and ceramics were sterilised by baking in aluminium foil at 500 °C for 3 hours. Amino acid standards were purchased from Sigma-Aldrich. AG® 50W-X8 resin was acquired from Bio-Rad. Sodium hydroxide and hydrochloric acid (37 %) were purchased from Boom and ammonium hydroxide (28-30 wt%) was obtained from Acros Organics. o-Phthaldialdehyde (OPA), N-acetyl-L-cysteine (NAC), sodium acetate trihydrate, sodium borate decahydrate as well as HPLC-grade water were bought from Sigma-Aldrich and methanol (absolute, HPLC-grade) was purchased from Biosolve Ltd.

3.3 Regolith simulation chamber

A stainless steel vessel was built that allowed up to seven sample cups to be cooled and simultaneously irradiated

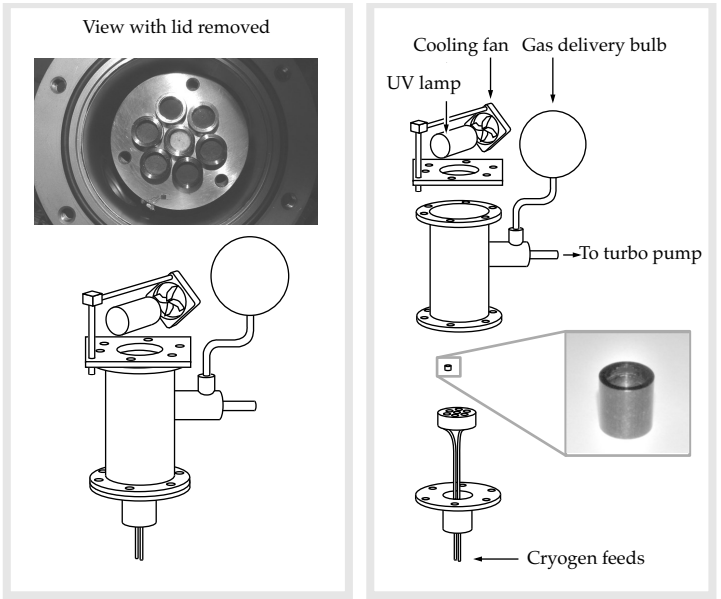

Fig. 3. The regolith exposure chamber, shown assembled in the lower left image and in its disassembled state in the right-hand image.

with UV light. The general form of the chamber is shown schematically in Fig. 3. A cylindrical block of brass held the seven stainless steel sample cups in six recesses around its perimeter with one recess in the centre. In this way all of the soil analogue samples had the same distance (~105 mm) from the discharge region of an external deuterium discharge lamp and thus received the same illumination intensity. The brass block was soldered to a coiled copper pipe that exited the chamber via a flange. A Dewar vessel holding pressurised liquid nitrogen was connected to this copper pipe, and a solenoid valve was used to modulate the cryogen flow so as to control the temperature of the brass block. The solenoid valve was controlled by a digital thermal controller wired to a platinum thermometer fixed to the sample holder block.

A turbo pump was used to evacuate the chamber and was backed by a two-stage rotary pump. No special precautions were taken to prevent oil back-contamination, as the analysis performed on the samples is insensitive to the hydrocarbons present in pump lubricants.

3.4 Lighting system

The UV light was provided by a high stability deuterium discharge lamp (Heraeus Noblelight, DX202). This lamp was held above the chamber's window inside an air-cooled shroud. A UV sensor (Solartech, model 8.0) was used to measure the intensity of the lamp's output in a narrow wavelength range (246 to 264 nm) and provided data traceable to a NIST standard source with an accuracy of around 10 %. To gain information about the irradiance of the lamp outside of this spectral range a deuterium lamp (Bentham Instruments Ltd, model R48) with a known spectral profile was used to calibrate the response of a monochromator equipped with a photomultiplier tube (PMT), which gave an output precision of around 10 mV for values covering the PMT's full-scale output of 0 to 300 mV. This monochromator observed the

deuterium lamp's output at wavelengths from 200 to 360 nm and the resulting irradiance data were scaled to match the power measured by the narrowband UV sensor. The resulting spectral profile is shown in Fig. 4, and the total flux of the lamp in the target plane was calculated to be 10^{14} photons cm^{-2} s^{-1}. The thick grey line shows unconfirmed data from the lamp's manufacturer and is for guidance only as those wavelengths lie outside the monochromator grating's range. For comparison, the irradiance expected on the equatorial surface of Mars at local noon is shown as a solid line, as predicted by the model of Patel *et al.* (2002) for a low-dust atmosphere. If the lamp's output is integrated, 85 % of the energy delivered by the lamp falls in the wavelength range of 190 to 325 nm, yielding an areal power in that range of 1 W m^{-2}. This evaluation criterion allows a comparison to be made with the natural lighting found on Mars; for our experiments the lamp yields a total intensity in the range of 190 to 325 nm that is one tenth of the intensity at the martian equator at local noon. It is also expected that amino acid degradation results from the shorter, rather than the longer wavelength light in that range. If the diurnal lighting variation is accounted for, one day of martian illumination corresponds to 80 hours of lighting from the deuterium lamp.

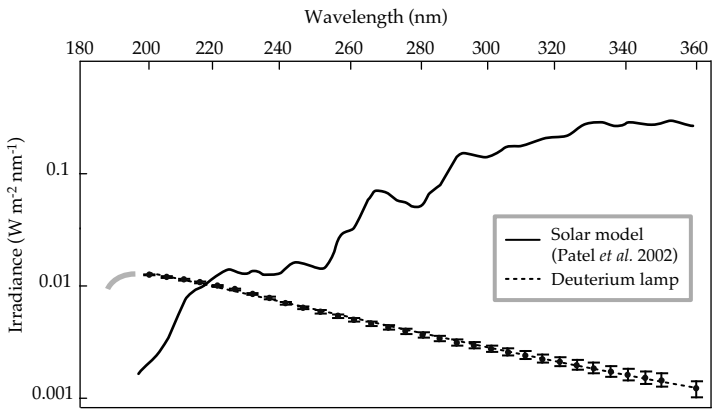

Fig. 4. The measured irradiance of the deuterium lamp in a plane 10 cm from the lamp's discharge point compared to the modelled irradiance at equatorial noon on Mars.

3.5 Mars simulation experiments

Prior to the experiments the stainless steel sample cups and the spoons used for filling the cups with the powdered analogues were cleaned with acetone and then with a solution of ethanol and demineralised water. After air-drying, the cups and spoons were sterilised by being baked at 300 °C for 3 hours. Six sample cups were filled with the chosen regolith analogues and one with the same amount of crushed Pyrex, serving as a control sample. The soil-containing cups were placed in the recesses around the perimeter of the brass sample holder, with the Pyrex control positioned in the centre. The chamber was then evacuated to the operating pressure of around 1×10^{-5} mbar in the course of a few hours.

Four experiments were performed; in experiment I, samples were exposed for 24 hours to UV irradiation in vacuum (~1×10^{-5} mbar). These conditions were similar to those employed by ten Kate *et al.* (2005) and thus provide an immediate com-

parison for the effect of embedding amino acids in a regolith. Secondly, an extended version of experiment I was performed, exposing fresh samples to 7 days of UV irradiation in vacuum (~1×10^{-5} mbar) and was named experiment II. Both of these experiments were conducted at room temperature (RT). A third experiment, illuminating new samples of the same materials for 7 days at a low temperature (210 K) was performed in a 7 mbar CO_2 atmosphere and is referred to as experiment III. In this last experiment, the turbo pump was shut off from the chamber and a glass vessel of known volume holding CO_2 (Praxair, 99.996 % purity) at a known pressure was connected to the chamber. This last experiment was designed to permit water vapour to accrete at the surface of the samples. At the chosen temperature of 210 K water ice has a smaller partial pressure than the ambient gas in the chamber and the vestigial amount of water outgassing from the stainless steel of the chamber would accrete onto the sample holders. By cooling the samples and in doing so, coating them with a thin water film, the work described in ten Kate *et al.* (2006) could be extended, in which the photolytic UV destruction rates of cold amino acid films were measured. In that work cooling of the samples led to a reduction in the rate of photolysis (ten Kate *et al.*, 2006) for glycine and in section 5.2 the influence of water films on the degradation of organic matter adhered to real mineral surfaces will be examined.

The photolytic destruction of thin films of amino acids in vacuum has been described earlier by ten Kate *et al.* (2005) and so an additional experiment (IV) was conducted to verify that there were no unwanted influences arising from the use of the irradiation chamber. A silicon disc was coated with a sub-micron layer of glycine and placed in the regolith illumination chamber. The disc was then illuminated with the UV lamp in vacuum. In contrast to the first three experiments, which used HPLC analysis, the amount of glycine on the silicon disc was measured with a Fourier transform infrared (FTIR) spectrometer (Excalibur FTS-4000, BioRad, range 4000 to 500 cm^{-1}, 4 cm^{-1} resolution), in the manner described in ten Kate *et al.* (2005). Briefly, this consists of measuring the integrated area of specific regions in the infrared absorption spectrum of the silicon disc and its film both prior to and after irradiation in the regolith experiment chamber. Then, by assuming first-order reaction kinetics (Cottin *et al.*, 2003) the destruction rate of the amino acid can be calculated from a linear fit through plots of the natural logarithms of the normalised integrated areas from the spectrum both before and after irradiation.

3.6 HPLC analysis

Each material was analysed through use of an established procedure (Zhao and Bada, 1995; Botta *et al.*, 2002) for separating and analysing amino acids in meteorite samples. This procedure requires that each sample was flame sealed in a test tube with 1 ml of water and boiled for 24 hours at 100 °C in a heating block. One of two equal parts of the supernatants was then subjected to a 6 N HCl acid vapour hydrolysis for 3 hours, 150 °C. Both the hydrolysed and the non-hydrolysed extracts of the samples were desalted on a cation exchange resin. The amino acids eluted from the resin with 5 ml of ammonium hydroxide. They were derivatised for 1 minute or 15

minutes with OPA/NAC. The fluorescent OPA/NAC amino acid derivatives were separated by HPLC coupled with an UV fluorescence detector (Shimadzu, RF-10AXL). HPLC analysis was carried out in a C_{18} reverse phase (250 × 4.6 mm) Synergi 4μ Hydro-RP 80A column from Phenomenex ®, with UV fluorescence occurring by excitation at a wavelength of 340 nm and emission at 450 nm. The conditions for amino acid separations for the mobile phase at 25 °C were as follows; the flow rate was set at 1 ml minute $^{-1}$, buffer A was 50 mM sodium acetate, containing 4 % methanol (v/v), and buffer B was methanol. The gradient used was 0 to 4 minute, 0 % buffer B; 4 to 5 minutes, 0 to 20 % buffer B; 5 to 10 minutes, 20 % buffer B; 10 to 17 minutes, 20 to 30 % buffer B; 17 to 27 minutes, 30 to 50 % buffer B; 27 to 37 minutes, 60 % buffer B; 37 to 49 minutes, 60 % buffer B; 49 to 50 minutes, 60 to 0 % buffer B; 50 to 60 minutes, 0 % buffer B. Amino acids were identified by comparing their retention time with known standards. The amino acid abundances (part per billion by weight) in the soil samples were calculated by comparing the integrated peak area, corrected for the abundances in the blank Pyrex sample, with the integrated peak area of known amino acid standards.

4. Results

4.1 Material characterisation

An investigation of the amino acid content in the two regolith analogues was made using HPLC. These materials were ana-

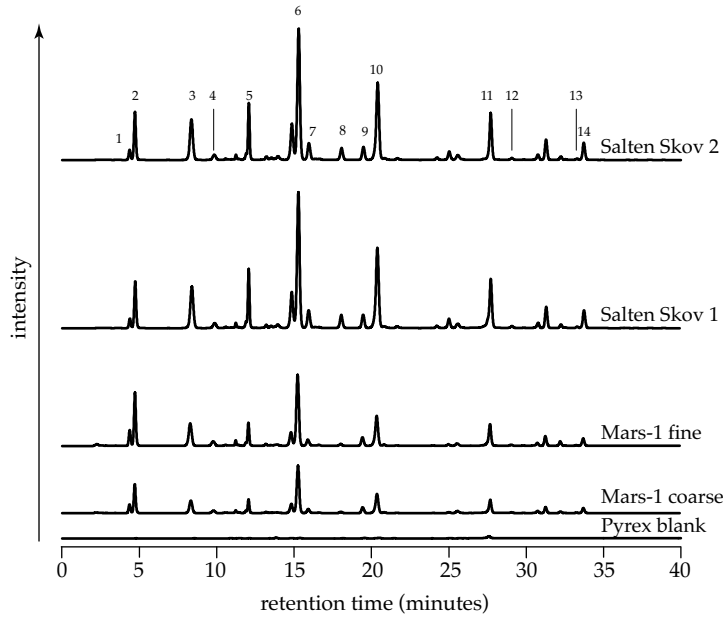

Fig. 5. The 0 to 40 minute region of the HPLC chromatograms for the un-irradiated materials. No peaks were detected outside this time period. OPA/NAC derivatisation (1 minute) of amino acids in the Mars-1 coarse material, Mars-1 fine grain sample, Salten Skov samples and blank are shown. The peaks were identified as follows: 1: D-aspartic acid; 2: L-aspartic acid; 3: L-glutamic acid; 4: D-glutamic acid; 5: D, L-serine; 6: glycine; 7: β-alanine; 8: γ-amino-n-butyric acid (γ-ABA); 9: D-alanine; 10: L-alanine; 11: L-valine; 12: D-valine; 13: D-leucine; 14: L-leucine. Other peaks are discounted, due to lack of signal, or ambiguous interpretation for the standards used.

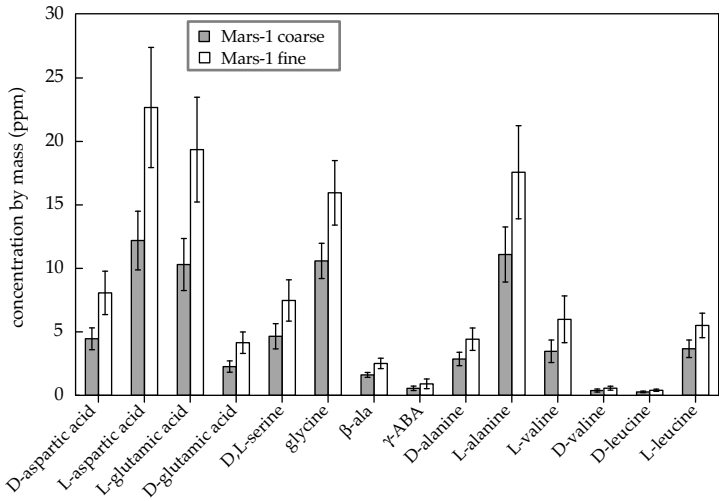

Fig. 6. Average absolute blank-corrected amino acid concentration in the unirradiated samples of coarse and fine-grained fractions of Mars-1.

lysed without any prior treatment, and were taken directly from the batches sent by their respective source institutes. Chromatograms for each of the materials used in this work are shown in Fig. 5.

The Mars-1 material was separated into two fractions, one having fine grains and one with coarser grains, as described earlier. Each of these fractions was sampled and analysed three times by HPLC using two different derivatisation pe - riods. The average of the data from those three analyses are shown as rectangular columns in Fig. 6 and the minimum and maximum values of the data are shown by the upper and lower ends of the capped vertical bars.

The concentration by weight of the detected amino acids dif - fers between the Mars-1 coarse and fine samples. Crudely, for a given amino acid, the concentration in the fine sample of Mars-1 is around one third greater than the concentration of that compound in the coarse sample. The near-uniformity of this relationship suggests that the organic content of the fine and coarse samples is a function of grain area. By contrast,

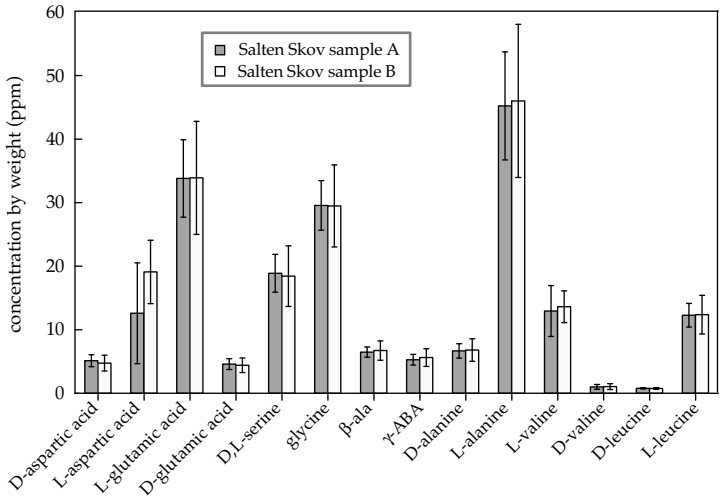

Fig. 7. Average absolute blank-corrected amino acid concentration in two samples of unirradiated Salten Skov material.

no variation could be seen in the Salten Skov material in two portions of the material taken from the top and bottom of the bulk. This is probably because the material used had already been sieved to yield a narrow grain size distribution and thus rendered homogenous, as is seen by the tightly clustered values for the mean concentration for each amino acid in Fig. 7. An identical processing sequence was used for this material as was used for the Mars-1 regolith and the rectangular columns in Fig. 7 show the average of all the data per sample. Again, the capped vertical bars indicate the span of the data.

The Salten Skov material does not have the same amino acid distribution as the Mars-1 analogue. Not only are the absolute concentrations of the detected amino acids higher by around a factor of 2 than in the Mars-1 regolith, but the Salten Skov material is richer in L-alanine, and deficient in L-glutamic acid, when compared to Mars-1. Despite their very different origins there are, however, common features in the amino acid make-up of the two soils that suggests that both Salten Skov and Mars-1 might have experienced a common contamination process, such as manual handling when they were collected. The ratio of L-valine/L-leucine in human sweat is around 2 (Hier *et al.*, 1946), in broad agreement with the ratio seen in both the Mars-1 and Salten Skov materials. If contamination from handling is neglected, amino acids may still arise in the Mars-1 soil as a result of abiotic processes in the production of fresh volcanic ash (Markhinin and Podkletnov, 1977) and the excavation site on Hawaii will in any case be exposed to aerosol-carried contaminants. The material excavated at Salten Skov has probably not experienced aeolian deposition, but will have had groundwater and readily soluble amino acids from bacterial metabolism and decay percolating through it.

Table 1: Showing the conditions and sample weights (mg) in each experiment.

Sample	Experiment type		
	I: 1 day UV, vacuum, ~300 K	II: 7 days UV, vacuum, ~300 K	III: 7 days UV, CO_2, 210 K
Pyrex blank	38.3	30.0	38.4
Mars-1 coarse	31.2, 31.3	30.3, 30.7	29.3, 30.2
Mars-1 fine	30.2, 29.8	30.1, 30.8	31.0, 33.2
Salten Skov A	35.5, 29.1	30.4. 33.1	29.6, 34.8

4.2 Mars simulations

Four different experiments were performed. In each experiment two samples of the Mars-1 material, and two samples of the Salten Skov soil were used to ensure higher accuracy. A Pyrex control sample was also exposed in the centre of the sample holder during each experiment. The weights of the samples were measured with a laboratory top-pan balance (Mettler AT200), and are shown in Table 1. Care was taken to ensure that the cups were not tilted or struck, so as to preserve the layer-like state of the powders within. The small quantities of material resulted in layers around 1 mm deep. For each experiment the same material was held in two diametrically opposed sample cups, hence two values are shown for each of the Mars-1 and Salten Skov weights in Table 1.

The conditions employed in the three experiments involving the irradiation of soils have been described in section 3.5. Before the data from those experiments are shown, the results from the fourth experiment are discussed. As described in section 3.5, a fourth test was performed to confirm that this particular experimental set-up could reproduce the degradation phenomena seen in earlier work using other equipment.

A thin film of glycine was prepared in the manner described by ten Kate *et al.* (2005), placed in the regolith irradiation chamber, and exposed to the UV lamp under a pressure of 10^{-6} mbar. The disc and its glycine coating were studied by FTIR prior to and after irradiation. From these data points the destruction rate for a thin film of glycine was found to be $2.6 \pm 5 \times 10^{-6}$ molecules s^{-1}, which is approximately a factor

Table 2. Absolute blank-corrected amino acid average concentration and data scatter from HPLC measurements in experiment I.

Amino acid	Fine Mars-1		Coarse Mars-1		Salten Skov	
	ppb	span	ppb	span	ppb	span
D-aspartic acid	10375	1018	8939	1119	9521	1071
L-aspartic acid	24164	2262	20989	1502	35404	4482
L-glutamic acid	18499	1801	15963	1483	43769	4936
D-glutamic acid	5113	621	4390	761	6846	933
D,L-serine†	6931	1364	5930	897	23037	2518
glycine	20764	2171	18542	2577	44047	5470
β-ala	4685	393	4128	398	9997	1112
γ-ABA	1678	182	1373	200	6660	746
D-alanine	6469	750	5717	568	10332	1646
L-alanine	17368	2026	15351	2038	54002	6976
L-valine	3676	3326	3402	2804	16393	6371
D-valine	600	451	524	285	1269	973
D-leucine	587	61	536	34	1518	304
L-leucine	5198	593	4597	379	16294	2151

†Enantiomers could not be separated under the chromatographic conditions.

Table 3. Absolute blank-corrected amino acid concentration and data scatter from HPLC measurements in experiment II.

Amino acid	Fine Mars-1		Coarse Mars-1		Salten Skov	
	ppb	span	ppb	span	ppb	span
D-aspartic acid	9947	1151	8315	710	7481	900
L-aspartic acid	27335	3056	22885	1921	38393	4442
L-glutamic acid	21299	2745	17770	1541	45993	5832
D-glutamic acid	4998	1219	4459	368	6108	1088
D,L-serine†	8777	1004	5757	3958	24920	2563
glycine	25140	1299	24024	1164	45284	4968
β-ala	5281	450	5320	428	10281	1279
γ-ABA	2240	302	1506	285	6193	940
D-alanine	6293	680	5699	531	9116	1064
L-alanine	20803	1502	18000	1112	56486	6817
L-valine	8007	4423	6142	3339	16655	14434
D-valine	336	228	376	177	915	485
D-leucine	436	66	397	87	959	144
L-leucine	5915	956	4784	786	17641	2763

†Enantiomers could not be separated under the chromatographic conditions.

of 2 larger than the figure calculated by ten Kate *et al.* (2005). This small difference can be attributed to the lack of data, as the fixed arrangement of the samples in the chamber did not allow in-situ measurements to be made of the film's IR transmission spectrum. In contrast, the equipment used by ten Kate *et al.* (2005) allowed a dozen or so transmission spectra to be recorded during the film's breakdown.

Table 4. Absolute blank-corrected amino acid concentration and data scatter from HPLC measurements in experiment III.

Amino acid	Fine Mars-1		Coarse Mars-1		Salten Skov	
	ppb	Span	ppb	Span	ppb	Span
D-aspartic acid	4345	784	6516	1621	5618	1057
L-aspartic acid	11552	2058	17583	4305	23828	4442
L-glutamic acid	9379	1614	14440	3552	31850	6001
D-glutamic acid	2175	445	3338	850	4403	1004
D,L-serine[†]	3644	479	5414	1390	15314	3516
glycine	7095	1265	10900	2749	20618	3682
β-ala	1751	307	2670	721	4744	884
γ-ABA	666	94	1699	436	3857	735
D-alanine	2392	425	3651	915	5617	1038
L-alanine	8104	1420	12383	3019	37181	7123
L-valine	6516	2460	7418	1435	19879	2540
D-valine	158	640	172	654	475	588
D-leucine	451	708	224	167	734	223
L-leucine	2245	1072	4000	964	12261	2262

[†]Enantiomers could not be separated under the chromatographic conditions.

In Tables 2, 3 and 4 the amino acid concentrations of the different analogues are shown for the first three experiments performed. The amino acid concentration by weight of each material, shown in the columns labelled 'ppb', is the average of data from the two samples of that analogue present in the chamber. The concentration shown for each of the three materials is an average of six HPLC measurements. The difference between the maximum and minimum values for the six concentration values for an amino acid in each material is tabulated in the columns headed 'Span'. Those values reflect the scatter in the concentration data and, given the complexity of the extraction and subsequent HPLC processes, should not be interpreted as an error in the sense of a random process occurring over many repeated identical trials.

Data for experiment I, consisting of exposure to UV light and vacuum at room temperature for one day are shown in Table 2. In Table 3, the data from experiment II, involving exposure to UV light and vacuum at room temperature for seven days are shown. Finally, in Table 4, the data from experiment III are listed, in which the samples were irradiated and cooled to 210 K in a CO_2 atmosphere.

For clarity, the shifts between the concentration of amino acids in the unirradiated samples and the concentrations in the soils in each of the three experiments (I, II, and II) are shown in Figs. 8 and 9 for the Mars-1 fine-grain analogue and the Salten Skov material respectively. The JSC Mars-1 coarse fraction data are not plotted, as they substantially follow the trends of the finer fraction.

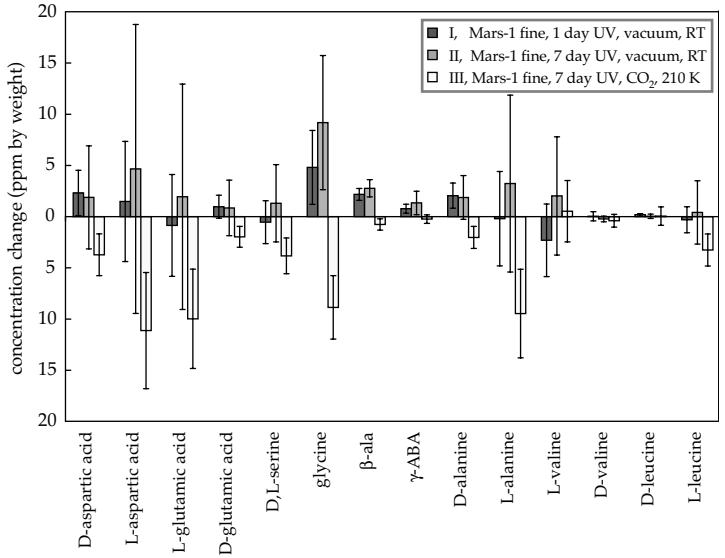

Fig. 8. The change in concentration in amino acids in the Mars-1 fine fraction resulting from experiments I, II, and III. An increase of certain amino acids can be observed after UV irradiation in vacuum at room temperature (RT). Enhanced destruction of D and L-aspartic acid, D and L-serine, L-glutamic, glycine, and L-alanine was observed in an experiment at 210 K and in a CO_2 atmosphere.

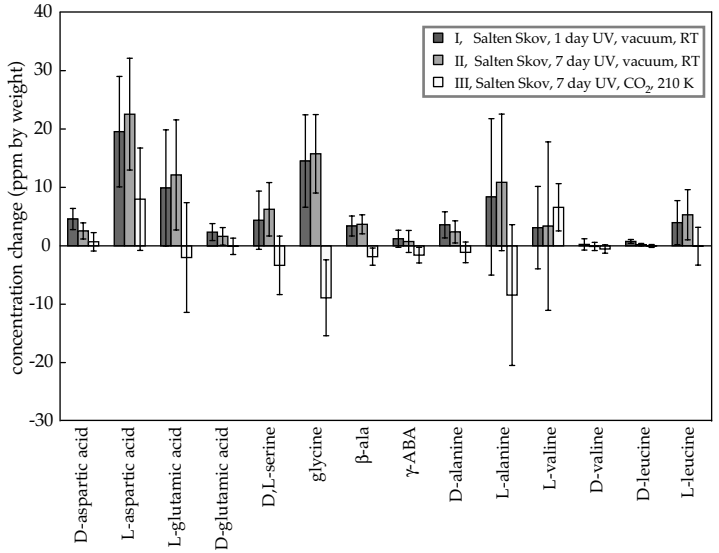

Fig. 9. The change in concentration in amino acids in the Salten Skov material resulting from experiments I, II, and III. An increase of certain amino acids was measured after UV irradiation in vacuum at room temperature. Enhanced destruction of glycine and L-alanine was observed in an experiment at 210 K and in a CO_2 atmosphere.

5. Discussion

The data shown in Figs. 8 and 9 appear to show three trends. Firstly, there is an apparent increase in the concentrations of certain amino acids as a result of exposure to vacuum and UV light. For the Salten Skov material the largest relative increase is seen for L-aspartic acid, which more than doubles in concentration when compared to its unirradiated concentration. The Mars-1 fine fraction displays broadly similar but smaller relative changes, with L-leucine doubling in concentration,

and the remainder rising in concentration by a lesser amount upon exposure to vacuum and UV light. No obvious sources of contamination were identified, and the same procedures were followed for analysis of pre-irradiated and post-irradiated samples, which ordinarily yielded values that were repeatable to a few ppm (Fig. 6). Secondly, the concentrations of the detected amino acids in the regolith samples do not change significantly when the UV exposure duration is changed from 1 day to 7 days, indicating that the process causing the rise in amino acid concentrations is rapid. Thirdly, in experiment III the concentrations of the measured amino acids after irradiation were uniformly lower than the concentrations of the amino acids recorded at the end of experiment II. This change is most pronounced in the Mars-1 data, which show a reduction in the amino acid concentration to levels, broadly, below that of the unirradiated samples. Experiments by ten Kate *et al.* (2006) demonstrate that cooling pure films of amino acids to 210 K slows down their rate of degradation by a factor of 7 or so, when they are exposed to a UV source. The lamp used in that work is the same model as used in the fourth experiment presented here, and it is therefore apparent that photolytic degradation cannot explain the absolute reduction in amino acid concentration that is seen in experiment III. A related experiment by ten Kate *et al.* (2006) shows that an ambient 7 mbar atmosphere of CO_2 at room temperature, makes no measurable change to the UV-induced degradation rate of a thin amino acid film. That study argues that no significant quantities of reactive species are generated within the gas around the samples, as the degradation rate is essentially unchanged from that seen for amino acids in a hard vacuum.

It is important to note that in experiment III only the sample holder was cooled, not the whole chamber. Therefore the gas within the chamber would have been substantially warmer than the 210 K of the brass sample holder and the soils. The difference between that study and the illumination of a soil is that in experiment III the organic matter is intimately connected to irregular mineral grains, which will scatter and absorb infalling UV light, rather than reflecting it. It is likely then that processes driven by UV photons, such as the mobilisation of electrons at a surface and the subsequent formation of trapped radicals, will proceed more effectively on UV absorbing mineral surfaces coated with water, than on a weakly absorbing or reflecting surface.

The apparent increase in amino acid concentrations as a result of exposure to vacuum and UV is worthy of extended discussion. Neither the Mars-1 nor the Salten Skov samples were cleaned in any manner. Thus it is likely that these materials contained organic contaminants from atmospheric aerosols, microbes from a variety of species, and bulk organic matter from the original excavation sites. Analysis of the JSC Mars-1 soil by Mendez *et al.* (2005) and Allen *et al.* (2000) showed the presence of fungi and culturable and non-culturable bacteria within it and it is possible that the Salten Skov material could also be host to bacterial or fungal spores. It is very likely that some of the apparent formation of amino acids, such as L-glutamic, L-aspartic, L-alanine, and so on, indicates the degradation of cell walls and the lysis of living bacteria or bacterial spores present in the regoliths. Certainly, these amino acids are present in the cell wall proteins of common

bacilli such as *E*. coli. (Howe *et al.*, 1965). To test the degradation hypothesis would require work perhaps involving some form of genetic or biomarker tracing. A similar rise is seen in the amino acid concentrations of the Mars-1 and Salten Skov material despite their different amino acid make-up in their unirradiated state. Therefore it might be argued that such a common change is the result of a common biological process, such as spore degradation.

5.1 Model of amino acid degradation within a regolith

The regolith analogues used in this work were exposed to the UV light generated by a deuterium lamp. No UV light with an intensity greater than 0.1 μW cm $^{-2}$ in the range of 245 to 265 nm penetrated shallow (~1 mm thick) layers of Mars-1 or the Salten Skov material when illuminated with a UV intensity of 500 μW cm $^{-2}$ from a xenon solar simulator. Thus, photolytic processes will only occur at the exposed surface of the regolith samples. If the powders are treated as spherical grains that are optimally packed, then the actual grain area that the radiation may strike is larger than the geometric cross-section of the sample cups. If the grains are assumed to be perfect absorbers, then only direct light from the lamp and radiation scattered from the sample cup walls can strike the regolith. If a vessel of radius R holds a powder of well-packed spheres with radius r, then only the upper hemispheres of the grains at the surface can be irradiated. Thus light penetrates only a distance r into the powder. The powdered sample has a known mass, m, and a bulk density ρ_{bulk}, and so the thickness, d, of the sample is given by equation 1.

$$d = \frac{m}{\rho_{bulk}\pi R^2} \qquad (1)$$

The sample holders have a cylindrical geometry, and so total area of the sample varies linearly with sample thickness. Thus, the ratio, A, of the irradiated area at the surface to the total shadowed area is given by equation 2.

$$A = \frac{r}{\left(\frac{m}{\rho_{bulk}\pi R^2}\right)} \qquad (2)$$

It will be assumed that all of the samples used have modal grain sizes of ~100 micron, as the difference between the coarse and fine Mars-1 materials appears to lie in the inclusion of large grains in the 'coarse' sample rather than the exclusion of finer material. The weights of the materials used in each experiment were listed in Table 1 and a nominal average bulk density, ρ_{bulk}, of 900 kg m $^{-3}$ will be assumed. The bulk density of Mars-1 can lie between 870 and 1070 kg m $^{-3}$ (Allen *et al.*, 1998). For the vessel (R = 5 mm) used to hold the powders, the fractional area, A, of a sample that receives direct radiation is of the order of 25 % of the total surface area in the sample. Thus, if the regolith and any incumbent organic contamination with a photolytic characteristic lifetime of τ are exposed to a photolytically degrading process, then the concentration, C, of that organic matter remaining after time t is simply

$$C = C_{(t=0)}\left[(1\text{-}A) + Ae^{-\frac{t}{\tau}}\right] \qquad (3)$$

The photolytic degradation rates of glycine and D-alanine are known from earlier experiments (ten Kate *et al.*, 2005) and so only these compounds will be discussed. D-alanine, with its half-life of 3 hours under martian equatorial noon-time conditions, should have been completely removed from the upper *A* fraction of the analogues used in this work during one day. In that time the overall concentration glycine would have only been reduced by around 13 %. Further irradiation for 6 days would not change the total amount of D-alanine in the regolith, as it will have been depleted from the region accessible to UV, whereas the overall concentration of glycine would fall to ~75 % of the original concentration. Given the accuracy and precision of the HPLC technique used, it is possible that this change would have been detected. The absence of a lowering of the amino acid concentrations in experiment II, suggests that either the grains stabilised surficial organic compounds against photolysis, or that the production of amino acids by the postulated breakdown of cell walls surpassed their photolytic removal.

5.2 Candidate photochemical processes

Several compounds and processes have been suggested as potential oxidising agents that are presumed to operate at the martian surface (Banin, 2005; Zent and McKay, 1994). It is worth examining some of these to assess whether the removal of amino acids in experiment III can be explained through the action of a reactive compound. For example, through photolysis water can form OH· radicals, which then can dimerise to hydrogen peroxide (H_2O_2) although other paths to its production are possible. The low thermal stability of H_2O_2 makes this a good candidate for the oxidation of matter at low temperatures and on Mars it may be stable at significant depths within a regolith column (Bullock *et al.*, 1994). The expected martian equilibrium surface adsorbed concentrations for H_2O_2 are of the order of 250 nmoles cm^{-3}, based on a production rate of around 5×10^{10} cm^{-2} s^{-1} (Bullock *et al.*, 1994). The formation of H_2O_2 is ultimately dependent on the concentration of water vapour in the atmosphere, and so it is possible to scale the production rate on Mars to the conditions present in the regolith illumination chamber. The chamber could be evacuated to a low pressure with the turbo pump. When the chamber was valved-off from the pump's inlet, the pressure in the chamber rose over the course of a day to an equilibrium value of around 10^{-2} mbar. The source of this vapour is presumed to be water vapour outgassing from the regolith and from the chamber walls. This last source is expected in stainless steel vacuum systems that have been opened to ambient air. The partial pressure of water in Mars' atmosphere at the surface is believed to be around 10^{-3} mbar, and so a crude estimate for the production rate of H_2O_2 in the chamber from water photolysis can be made by comparing the optical path length of the chamber to the effective column height of Mars' atmosphere. By doing so, a formation rate of ~10^{6} cm^{-2} s^{-1} is found, which results in a fractional areal coverage rate of one part in 10^{8} per day for each regolith sample in the chamber. Changes in the amino acid concentrations over the course of one day would be undetectable with the HPLC method described in this work.

Water may also play a less direct role in forming oxidising agents. It has been shown that the interaction of oxygen with UV irradiation (Oró and Holzer, 1979) leads to the degradation of amino acids, but oxygen is a minor constituent of the martian atmosphere. The presence of water frosts on mineral surfaces is pertinent, as the exposure of thin water frosts on iron-bearing minerals to UV has been shown to cause the release of oxygen upon warming (Huguenin *et al.*, 1979), arising from the formation of a condensed oxidising agent at the mineral surface. Later experiments with feldspar by Yen *et al.* (2000) demonstrate that superoxide radicals such as O_2^- are formed through the combination of cold mineral surfaces (-30 ºC), Mars-like UV lighting, free oxygen, and low concentrations of water. The quantum efficiency for this process has been estimated by Yen *et al.* (2000) as being 10^{-6} radicals photon^{-1}, who also predict a production rate of 10^7 cm^{-2} s^{-1}. It is appropriate to ask if these UV-generated radicals are therefore responsible for the degradation seen in experiment III. Our experiments with cooled mineral surfaces under UV irradiation were performed in an ambient gas with a mixing ratio of oxygen no greater than 50 ppm by volume according to the manufacturer's datasheets, this is a concentration around 20 times smaller than in the martian troposphere. Thus, scaling for the lower illumination levels and oxygen content in the regolith chamber, approximately 10^4 radicals cm^{-2} s^{-1} would be expected to form on the surfaces of the regolith samples studied in this work. In the course of one day O_2^- radicals may have an areal coverage of 1 part in 10^{10} of the exposed regolith. The above calculations are based on the amount of gaseous oxygen in the CO_2 atmosphere of experiment III and neglect the potential for oxygen to be formed from the decomposition of adsorbed water by photolysis at the cold mineral surfaces of experiment III. It is therefore still possible that the amino acid degradation seen in experiment III is driven by oxidative attack from O_2^- radicals and perhaps other photochemical species, formed within the adsorbed water layers bound to the surfaces of the soil grains that are illuminated by energetic UV.

Water can also play a role as a mediating agent for the mobilisation of acids generated through nitrogen and sulphur oxidation (Quinn *et al.*, 2005d). In the work presented here neither of those compounds was present in the gas-phase at levels above a few ppb in any of the experiments and so dry-acid deposition by aerosols is not expected. However, water adsorbed at the surface of a mineral can leach soluble species from the rock, leading to a situation in which Fe(II) ions generate OH· ions via the photo-Fenton reaction of H_2O_2 with UV. This process is well studied on Earth (Southworth and Voelker, 2003) and in martian scenarios (Benner *et al.*, 2000, Möhlmann, 2005). Thus, a plausible pathway for the formation of a vigorous reactive species is present in experiment III, involving the presence of water adsorbed onto mineral surfaces. In experiment III the samples were cooled to 210 K in the presence of water with a partial pressure of around 10^2 mbar, around an order of magnitude higher than the partial pressure of water in the near-surface atmosphere of Mars (Schorghofer and Aharonson, 2004). A theoretical model presented by Möhlmann (2004) indicates that a few monolayers of water would be ubiquitous on exposed martian surfaces,

with the total thickness fixed by the partial pressure of water. We therefore suggest that the samples within experiment III were coated with a quasi-liquid water layer, permitting the generation of the OH· radicals to occur within that adsorbed water. The exact chemical path for its formation is not decidable from our data, and several candidate pathways are available aside from those indicated in section 5.2, such as the photo-Fenton reaction on iron-bearing minerals (Möhlmann, 2004).

5.3 Comparison to the martian environment

The martian surface experiences lighting spectra and material transport processes that are difficult to emulate in a laboratory. To first order, we assume that the spectrum of the light can be modelled with a fixed profile. In the apparatus used to illuminate the samples the lamp produces an integrated power in the wavelength range of 190 to 325 nm that is around one tenth of the intensity expected to occur in that band at noon in the equatorial regions of Mars. Furthermore, the surface of Mars is not a static environment and the action of wind, saltating grains, and sporadic meteorite impact, all act to till the regolith over different timescales. Thus the uppermost UV-exposed regolith grains will be progressively mixed into the ground. If a grain is removed from the surface by some form of gardening in a time that is shorter than the organic matter's photolytic lifetime, then there will be no sharp boundary between the UV-cleansed upper surface and deeper layers.

A further relevant point concerns the use of constant temperatures for periods greater than one day, of ~300 K in experiments I and II, and 210 K in experiment III. These conditions do not accurately reflect the equatorial diurnal temperature cycle seen on Mars, as the warming and cooling cycle experienced by the martian surface throughout a full day is not simulated. This is an important factor as the reactivity of chemical species formed either through photochemical or photolytic pathways on the martian surface will be influenced by the ambient temperature. The longevity of such species (H_2O_2, etc.) will also depend on the surface temperature and their abundance will be influenced by the porosity of the regolith. It is possible that a balance will be struck between the rate at which a species may decompose during the day, and the rate at which they may condense during the night. We do not mimic other processes occurring on Mars, such as burial by dust at sundown, that could lead to the preservation of oxidising agents formed through interaction with water.

6. Conclusion

We have performed analyses of two martian regolith simulants and have quantified their amino acid content. In doing so we have obtained data that are useful to biological, chemical, and physical studies of analogues for martian surface materials. If biological processes occurred on Mars in the past, they may have been exposed to climatic conditions different from those currently seen on that planet. The chemical signatures from these processes, and the materials brought by meteorites throughout Mars' history, are subject to a number of

destructive processes that operate at different timescales and in the presence of different materials. We have studied the effect of an important process, UV radiation, on two soil analogues. Exposure of these materials to conditions of vacuum and energetic UV appears to generate higher concentrations of amino acids within the materials. This process is rapid and repeatable in all the samples used, with exposures of one day yielding results similar to those arising from seven days of irradiation. It should be noted that seven days of irradiation in the laboratory is equivalent to the light received during 2 full days on Mars. It is postulated that this in-situ formation results from the degradation of extant biota within the soils, and the fingerprint of amino acids present is suggestive of the degradation of cell walls, as indicated in section 5.

With the method used, photolysis of the amino acids present in the soils, or generated through cell destruction was not detected. The shallow samples permit a significant fraction (of order 30 %) of the material to be irradiated, a value comparable to the precision of the HPLC process employed. Separately, we have demonstrated that a pure amino acid film can be degraded within the experimental chamber when the sample is lit by the UV lamp used in the experiments described here. The degradation rate from that measurement is in line with expectations from earlier work (ten Kate *et al.*, 2005) and therefore photolytic degradation should occur in the regolith samples exposed to UV, but other factors dominate the changes seen in the amino acid concentrations.

Cooling of the regolith samples to 210 K and simultaneous exposure to an atmosphere of carbon dioxide leads to the removal of amino acids when compared to unirradiated samples. It is probable that adsorbed water on the mineral surfaces is key to the generation of reactive species on the grains, and the subsequent degradation of the amino acid content within the soil, as is discussed by Quinn (2005d) and Zent and McKay (1994). While the details of this process are not visible from this work, it is worth noting that the amino acid degradation caused by cooling in the presence of background water is comparable in magnitude to the degradation expected by photolysis in the same period, see section 5.1.

If the apparent formation of amino acids in regolith simulants is taken at face value, there are implications for the use of these and other analogues in future. The diverse nature of the planetary research community means that a single material cannot reasonably represent the wide range of physical and chemical properties that are pertinent to martian science. A specific and timely concern is the nature of analogues that are appropriate for forthcoming missions that will engage in biological studies of in-situ and returned martian samples. For example, it is conceivable that materials used in simulations of a sample-return mission would, for purposes of verifying the curation and dispersal procedures, be subject to the same planetary protection regulations as a real sample (Rummel, 2001). As a part of such a process, qualification samples with no detectable organic content would be needed. While the physical properties (such as grain size distribution and so on) of an analogue can be controlled relatively easily, it is difficult to conceive of a process that would remove extant biota and

their corpses from a regolith analogue without changing the mineralogy of the material. Techniques employed in spacecraft sterilisation processes such as heat-sterilisation, irradiation with ionising particles and quanta, and exposure to oxidising gasses and plasmas, are unable to remove significant quantities of organic matter from a material. Thus, it would be desirable to establish a database of analogues for planetary regoliths, which are separately designed for chemical, biological, and engineering studies. We have demonstrated that an analogue, such as Mars-1, designed to be a spectral and physical match to a nominal average martian soil is inappropriate for a life-science study in its raw state.

Acknowledgements

JRCG is supported by grant MG058 from the SRON National Institute for Space Research, ILtK is supported by the BioScience Initiative of Leiden University, ZM is supported by Fundação para a Ciência e a Tecnologia (scholarship SFRH/BD/10518/2002), PE is supported by grant NWO-VI 016.023.003. We thank Zan Peeters for his help with the HPLC analyses and the clarity of this manuscript was improved by constructive comments from A. J. Jull, and the reviewers M. Sephton and C. McKay. Oliver Botta is thanked for his insight into HPLC processing.